YCRETS 2023
YOUNG CONCRETE RESEARCHERS, ENGINEERS & TECHNOLOGISTS SYMPOSIUM

CEMENT & CONCRETE SA

Hardened properties of 3D-printed limestone calcined clay cement concrete

Kamoru A. Ibrahim*, Mustapha B. Jaji, Gideon P.A.G. van Zijl, and Adewumi J. Babafemi*

Department of Civil Engineering, Stellenbosch University

*Corresponding author. E-mail address: kaibrahim@sun.ac.za & ajbabafemi@sun.ac.za

Abstract

The emergence of a highly productive construction technology named 3D printed concrete (3DPC) is a breakthrough in the construction industry due to its ability to conserve natural resources, reduce waste, and minimise time and costs associated with the construction of concrete infrastructure. This study investigates the performance of fibre-reinforced 3DPC made with limestone calcined clay cement (LC^3) to minimise the detrimental environmental footprint of ordinary Portland cement. LC^3 has been a promising supplementary cementitious material showing better performance in terms of strength development, compared to Portland cement and other blended cements. The mechanical response of LC^3 3DPC reinforced with micro synthetic polypropylene fibre under compression and splitting tensile loading including the modulus of elasticity is examined. The test results reveal that the anisotropic phenomenon was pronounced in mechanical characterisation of the 3D-printed specimens when subjected to loading conditions in different orientations. The peak load values of cylindrical specimens is lesser than that of cubic specimens, having mean strength ratios of 73% and 88% for compression and splitting tension, respectively. Finally, the relationship between the mechanical strength of both the cast and printed specimens cured for 28-day in a climate-controlled room at 23°C (± 2°C) and 65% (± 5%) relative humidity is presented.

Keywords: 3DPC, LC^3, compression, modulus of elasticity, splitting tensile

1. INTRODUCTION

The property of extrusion-based 3D printed concrete (3DPC) is investigated on both the micro- and macro-scales. The macro-scale: compressive strengths (cubes; f_{cu} and cylinders with slenderness equal to two; f_c geometries) are key material parameters in the analysis of concrete structures, which are conventionally utilised as a quality control parameter of concrete and to evaluate the structural application class. Other parameters such as modulus of elasticity (*E)*, tensile strength (f_t), and flexural capacity ($f_{flex.}$) are related to compressive strength and cannot be neglected when determining the ultimate load-carrying capacity of concrete elements. A multi-directional mechanical performance is studied in 3DPC, due to its anisotropic properties, i.e., a 3DPC element has different orthotropic mechanical capacities depending on the testing direction. This makes it different from monolithic conventional concrete structures where the structural integrity tests are normally done in one direction [1, 2].

Unlike the conventional construction method of cast-in-place concrete, 3D concrete printing (3DCP) is an emerging technique for digital fabrication that produced free-form structures and structures of complex geometries without moulds/formwork and other special tools [3]. This promotes architectural expression, where the production costs become independent of the produced structural components' quantity, shape, and complexity [4]. However, high cement content is required for the extrusion process of 3DPC and its sustainability benefits in terms of free forms and materials efficient design might be affected. Hence, the addition of limestone and calcined kaolinitic clay (naturally available supplementary cementitious materials) sufficiently reduced the clinker content of digital concrete; saving embodied carbon footprints, energy consumption, and cement/concrete production cost [5–7].

Many studies have attempted to utilise a combination of limestone powder and calcined kaolinitic clay to develop printable cementitious materials [8–10]. Their findings showed comparable mechanical properties to those of ordinary Portland cement (OPC) and Portland pozzolanic cement (PPC), and the improvement of some durability aspects. Limestone calcined clay cement (LC^3) is an intrinsic rheology modifier and pozzolanic material, which releases carbo-aluminate hydrate when calcite reacts with tricalcium alumina in the pore solution. Due to these actions, the capillary pores are filled, thereby reducing the porosity of cement-based materials and enhancing the mechanical performance at later ages [7, 8, 11].

In this study, the influence of limestone calcined clay (LC^2) on the mechanical properties of fibre-reinforced 3DPC (FR-3DPC) tested in a compressive setup was investigated by measuring the compressive strength, the splitting tensile strength, and the elastic modulus. Seven (7) concrete cubes (mould-cast) and thirty (30) cylindrical (10 mould-cast and 20 printed (10 D1 and 10 D3)) specimens were prepared and tested in the laboratory in this investigation.

2. EXPERIMENTAL FRAMEWORK

2.1. Experimental Materials

Pretoria Portland cement (PPC) Suretech clinker (CEM I 52.5 N) conforming to SANS 50197-1 [12], LC^2, and gypsum were used as raw materials for this study. Natural Malmesbury sand with fineness modulus of 2.12 and 4.75 mm nominal maximum size was utilised to improve the self-supporting behaviour of the material through mechanical occlusion. The particle size distribution curve of the sand and binders, as obtained from sieve analysis and laser diffractometry (Mastersizer 2000 and Hydro 2000SM), respectively, is shown in Fig. 1 with the mean particle size (D_{50}) of 307.28 μm, 19.36 μm, 18.81 μm, and 234.53 μm for sand, CEM I 52.5 N, LC^2, and gypsum, respectively. LC^2 has a relatively finer-grained structure than CEM I. Normal-modulus polypropylene (PP) fibre with its properties illustrated in Table 1 was incorporated in the 3DPC to control plastic shrinkage cracking and minimises brittleness [13]. The mixing water was added to the dry mixture, with a liquid Chryso Quad 20 viscosity modifying admixture (VMA) and high-efficiency Chryso Premia 310 superplasticiser (SP) for tailoring and optimising the rheological properties of ternary blended concrete to meet the 3DPC performance requirements. The chemical properties of the clinker (Portland cement) and other raw materials were obtained by X-ray fluorescence spectrometry (XRF) and are presented in Table 2, and the mix design of LC^3 FR-3DPC is shown in Table 3.

Table 1: Properties of the micro-synthetic fibre

Description	Young's modulus	Yield stress	Diameter	Length	Aspect ratio
PP	3 GPa	300 MPa	30 μm	6 mm	200

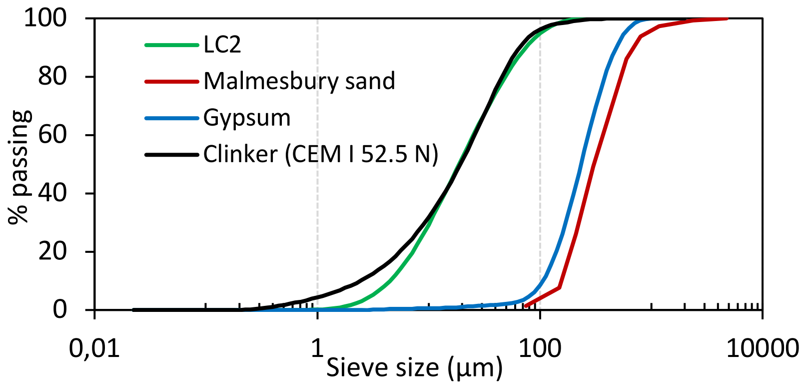

Fig. 1. Particle size distribution of LC^2, Malmesbury sand, Gypsum, and CEM I 52.5 N

Table 2: Chemical composition of cement and other raw materials

% Weight	Al_2O_3	CaO	Fe_2O_3	K_2O	MgO	Na_2O	SiO_2	TiO_2	LOI	Other
Clinker	4.08	62.92	3.16	0.57	1.00	0.18	19.90	0.23	5.08	2.88
LC^2	13.32	17.90	1.24	2.03	0.77	0.24	49.64	0.56	14.57	0.05
Gypsum	0.21	13.17	0.05	0.06	0.14	0.06	57.95	0.03	11.24	17.09

Table 3: Materials mix constituent proportioning (kg/m^3)

Mixture	Clinker	LC^2	Gypsum	Sand	Water	SP	VMA	PP
LC^3 FR-3DPC	381.9	343.7	38.2	1229	343.7	7.637	2.291	9

2.2. Experimental Methods

The 3D concrete mix design approach developed at the Structures and Building Materials Laboratory of Stellenbosch University (S&BML-SU) was modified for LC^2 inclusion. Mixing was done mechanically in a Hobart concrete mixer in the following order: dry mixing of aggregate and binders, mixing water addition, then the addition of admixtures (SP and VMA), and lastly, PP. Specimens for hardened properties were cast and compacted using an electro-mechanically driven vibration table, taken to the climate control room, and stripped after 24 hours. The printing technique adopted is extrusion-based using a gantry-type 3D printer, which operates in three translational degrees of freedom with a build volume of roughly one cubic metre (1 m^3) coupled with a concrete pump and circular nozzle of 25 mm diameter. The printing parameters selected, and the procedures followed to attain it were aligned with those reported by Ibrahim et al. [14]. The printing (rectangular solid object which is schematically represented in Fig. 2 with geometry) and curing for the cast and printed samples were made in a climate-controlled room at a temperature of 23°C (± 2°C) and 65% (± 5%) relative humidity.

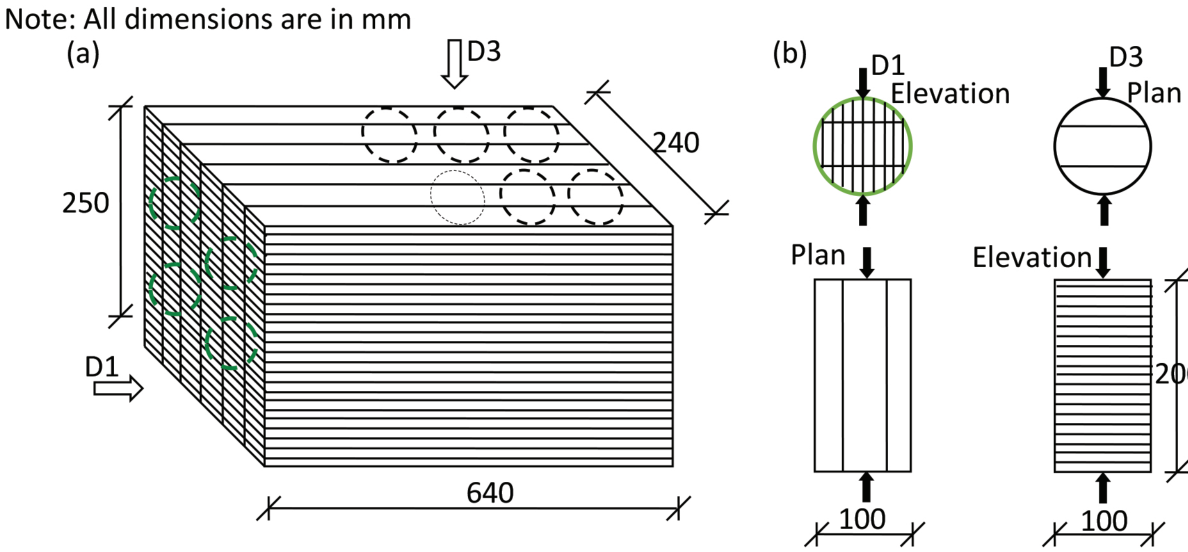

Fig. 2. The schematic representations of printed (a) object and (b) specimens: D1 & D3

2.3. Experimental Testing

Compressive strength test: The strength evolution characterisation for compressive (f_{cu}, cube & f_c, cylinder) strengths on the cast and printed (cored) specimens were executed after 28 days of curing using a 2 MN King Test Contest press machine at loading rates of 180 kN/min and 90 kN/min for cubes and cylindrical specimens, respectively, until failure adhering to BS EN 12390-3 [15] and ASTM C39 [16]. The test specimens were 100 mm cubes (cast) and 100 mm diameter × 200 mm long cylinders (cast and printed). Printed specimens were cored in two directions: D1 and D3 (see Fig. 2) in longitudinal and perpendicular to the printing direction, respectively.

Splitting tensile strength test: The splitting tensile test (f_{st}, cube & f_{sti}, cylinder) was performed on 100 mm cubes and 100 mm diameter x 200 mm height cylindrical specimens after 28 days of curing. The specimens were tested in a Zwick Z250 material testing machine at loading rates of 1.0 mm/min and 0.75 mm/min for cubes and cylinders, respectively, in accordance with BS EN 12390-6 [17].

Modulus of elasticity: Young's modulus (E) characterisation was conducted on 100 mm diameter x 200 mm height cylinders (cast and printed specimens) after 28 days of curing as per ASTM C469/C469M-14 [18]. Three linear variable differential transducers (LVDTs) with a 70 mm gauge length are circumferentially arranged at 120° intervals. Then, the testing was conducted using a 2 MN King Test Contest press machine at a loading rate of 90 kN/min with a 2 MN loadcell, loaded uniaxially up to 40% of their ultimate compressive capacity, and measurements were taken through an HBM Spider8 data acquisition system.

3. RESULTS AND DISCUSSION

3.1. Compressive Strength

The results of the compressive strength tests (f_{cu} & f_c) of LC^3 FR-3DPC specimens are depicted in Fig. 3. The mould-cast cylindrical specimens had an average strength of 73% of the cube's strength. In comparison to the printed specimens, the percentage decrease in strength are 3% and 9% for D1 and D3, respectively. This aligns with the anisotropic mechanical behaviour of 3DPC reported by van den Heever [19]. The increase in strength of the cast specimens is attributed to the restraining of the crack expansion, which reduced the stress concentration at the crack tip due to the presence of fibres. Several micro-cracks and the fibres bridge across the micro-cracks are observed in the concrete volume, making the failure mode change from fragile/brittle to ductile. Table 4 summarises the mechanical properties of the LC^3 FR-3DPC obtained from compressive strength, splitting tensile strength, and modulus of elasticity tests, with a minimum of three specimens tested for the observation. There is insignificant variation in the strength results of all specimens tested, showing the coefficient of variation (CoV) for all the results obtained to be less than 10%, indicating reasonable repeatability, consistency, and accuracy [14].

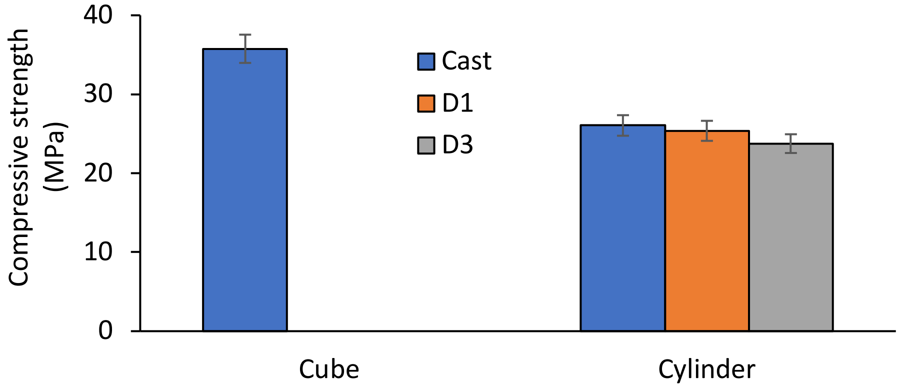

Fig. 3. Compressive strength development of LC^3 FR-3DPC specimens after 28 days curing

Table 4: Average mechanical properties of LC^3 FR-3DPC at 28 days curing age with CoV and number of specimens tested in brackets.

Specimen type	f_{cu} (MPa)	f_c (MPa)	f_{st} (MPa)	f_{sti} (MPa)	*E* (GPa)
Cast	35.76 (0.031; 4)	26.05 (0.030; 4)	3.27 (0.101; 3)	2.86 (0.048; 3)	21.43 (0.011; 3)
D1	–	25.37 (0.052; 4)	–	1.70 (0.050; 3)	18.77 (0.028; 3)
D3	–	23.75 (0.032; 4)	–	2.64 (0.028; 3)	16.09 (0.036;3)

3.2. Splitting Tensile Strength

Fig. 4 depicts the results of the splitting tensile strength for LC^3 FR-3DPC mixture with the specimens undergo pure tensile stress when subjected to a compressive force applied to a narrow region along its length at 28 days testing. The mean strength of 88% of the cube's strength is achieved for cylindrical cast specimens, indicating higher strength values recorded for cubic specimens when compared with cylindrical specimens, which is conformed to BS EN 12390-6 [17]. Also, the percentage decrease between the cast and D1 orientation is relatively large compared with D3, showing a significant difference between the specimens with 41% and 8% for D1 and D3, respectively. The presence of fibres influences the failure mode in cast and D3 specimens with the avoidance of sudden failure due to fibre bridging effect.

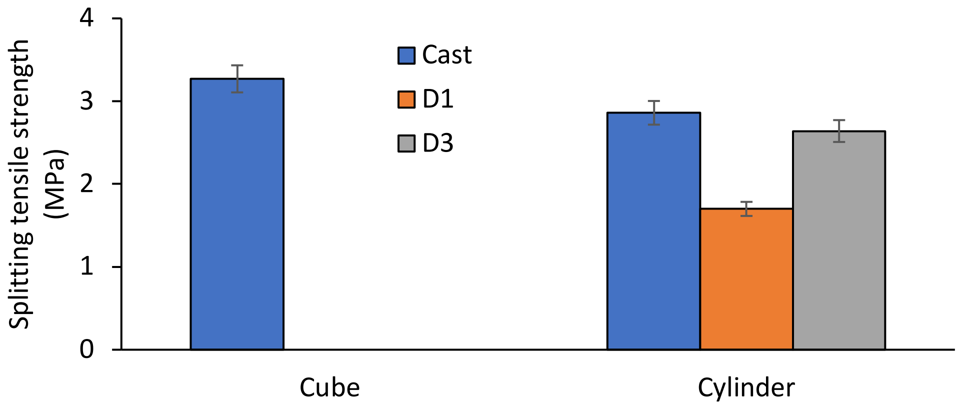

Fig. 4. Splitting tensile strength results and failure patterns for LC^3 FR-3DPC specimens at 28 days of curing

3.3. Modulus of Elasticity

The modulus of elasticity results of LC^3 FR-3DPC mix are presented in Fig. 5 and summarised in Table 4. It is evident that a higher value was recorded for the mould-cast specimens. In comparison, the percentage decrease between cast and printed specimens is 12% for D1 and 25% for D3. This significant difference might be due to the presence of air voids (increased porosity) between the deposited filament layers. Modulus of elasticity is one of the crucial material parameters for structural analysis, which is influenced by various factors such as the nature and compatibility between the matrix and filler, the filler distribution in the matrix, and interfacial structure and morphology [20].

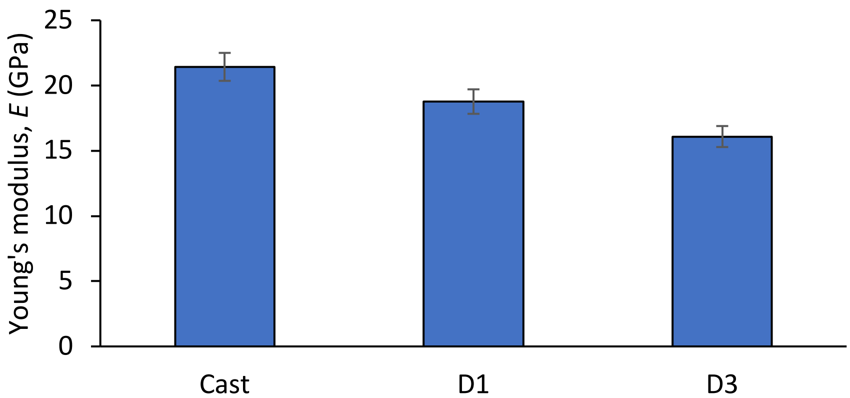

Fig. 5. Young's modulus results for LC^3 FR-3DPC specimens at 28 days of curing

4. CONCLUSIONS

The present study examined the effect of LC^3 on mechanical properties of FR-3DPC using cubes and cylindrical specimens. Based on the experimental observations, the following conclusions are drawn:

- The mean compressive strength of cylindrical specimens is 73% of the mean compressive strength of cubic specimens. This is ascribed to the difference in aspect ratio of specimen height to width of 2 for cylinders and 1 for cubes, and associated confinement in the cubes. The mean splitting tensile strength of cylindrical specimens was 88% of that of cubic specimens.
- Highest strength (compression and tension) and stiffness (Young's Modulus) were exhibited by mould-cast specimens. This could be ascribed to lower porosity and smaller pore size of cast specimens, compared with specimens extracted from 3D printed concrete.
- Fibres influence the post-peak mechanical behaviour of LC^3- based 3D printed concrete. This is ascribed to the fibre crack bridging effect. D3 splitting tensile specimens remained intact after registering their peak resistance.
- Anisotropic mechanical behaviour of LC^3 FR-3DPC was demonstrated for printed specimens in compression, splitting tension, and Young's modulus with the highest strength values recorded in D1 and D3 orientations for compression and Young's modulus, and splitting tension, respectively.

ACKNOWLEDGEMENTS

The first and second authors express their gratitude to the Tertiary Education Trust Fund (TETFund) under the Federal Ministry of Education, Nigeria for their financial support. The authors also thank Kaolin Group (Pty) Ltd, South Africa for providing the LC^2. Constituent materials were supplied in-kind by SAPY Corehfil Polypropylene fibres, PPC, and Chryso Cape Town, South Africa.

REFERENCES

[1] Cho, S., *"Rheo-mechanics and Foam Stability of 3D Printable Foamed Concrete with Nanoparticle Incorporation",* PhD Dissertation in Engineering, Stellenbosch University, South Africa, (2021) 134pp.

[2] Panda, B., Paul, S.C. & Tan, M.J., Anisotropic mechanical performance of 3D printed fiber reinforced sustainable construction material. Mater. Lett., 209: (2017) 146–149.

[3] Weger, D. Lowke, D. and Gehlen, C., 3D printing of concrete structures using the selective binding method – Effect of concrete technology on contour precision and compressive strength, 11th fib International PhD Symposium in Civil Engineering, The University of Tokyo, Tokyo, Japan, (2016) 8 pp.

[4] Nematollahi, B. Xia, M. and Sanjayan, J., Current progress of 3D concrete printing technologies, in: Proceedings of 34th International Symposium on Automation and Robotics in Construction, Taiwan, (2017) 260–267.

[5] Ruan Y, Jamil T, Hu C, Gautam BP, Yu J., Microstructure and mechanical properties of sustainable cementitious materials with ultra-high substitution level of calcined clay and limestone powder, Construction and Building Materials, 22: 314, 125416, (2022) 8 pp.
[6] Mohan MK, Rahul AV, Van Tittelboom K, De Schutter G., Rheological and pumping behaviour of 3D printable cementitious materials with varying aggregate content, Cem. Concr. Res. 2021; 139, 106258, https://doi.org/ 10.1016/j.cemconres.2020.106258.
[7] Scrivener K, Martirena F, Bishnoi S, Maity S., Calcined clay limestone cements (LC^3), Cem. Concr. Res. 2018; 114: 49 – 56, https://doi.org/10.1016/j.cemconres. 2017.08.017.
[8] Chen, Y. Figueiredo, S.C. Li, Z. Chang, Z. Jansen, K. Copuroglu, 0. Schlangen, E., Improving printability of limestone-calcined clay based cementitious materials by using viscosity modifying admixture. Cem Concr Res.; 132: 106040. (2020) 18 pp.
[9] Beigh, M.A.B. Nerella, V.N. Schröfl, C. Mechtcherine, V., Studying the Rheological Behavior of Limestone Calcined Clay Cement (LC^3) Mixtures in the Context of Extrusion-Based 3D-Printing. In: Bishnoi, S. (eds) Calcined Clays for Sustainable Concrete. RILEM Bookseries, vol 25. Springer, Singapore, 2020; https://doi.org/10.1007/978-981-15-2806-4_26.
[10] Reißig, S. Nerella, V.N. Mechtcherine, V., Material Design and Rheological Behavior of Sustainable Cement-Based Materials in the Context of 3D Printing. In: Buswell, R., Blanco, A., Cavalaro, S., Kinnell, P. (eds) Third RILEM International Conference on Concrete and Digital Fabrication. DC 2022. RILEM Bookseries, vol 37. Springer, Cham. 2022; https://doi.org/10.1007/978-3-031-06116-5_65.
[11] Gunnelius, K.R. Lundin, T.C. Rosenholm, J.B. Peltonen, J., Rheological characterization of cement pastes with functional filler particles, Cem. Concr. Res. 65, (2014) 1–7.
[12] SANS 50197–1; South African National Standard; Cement - Part 1: Composition, specifications, and conformity criteria for common cements, 2013.
[13] Van Zijl, G.P.A.G., Kruger, P.J., Cho, S., Zeranka, S., 3D printing polymer fibre concrete. In: Proceedings of the International Inorganic-Bonded Fiber composites Conference. 23–26 Oct 2018, Cape Town, South Africa, (2018) 5–14.
[14] Ibrahim K.A, van Zijl G.P.A.G. Babafemi A.J., Influence of Limestone Calcined Clay Cement on Properties of 3D Printed Concrete for Sustainable Construction, Journal of Building Engineering, (2023), 34 pp, doi: https://doi.org/10.1016/j.jobe.2023.106186.
[15] BS EN 12390-3; Testing Hardened Concrete Compressive Strength of Test Specimens. The British Standards Institution: London, UK, 2019.
[16] ASTM C39/C39M-18; Standard Test Method for Compressive Strength of Cylindrical Concrete Specimens; ASTM International: West Conshohocken, PA, USA, 2018.
[17] BS EN 12390-6; Testing Hardened Concrete Tensile Splitting Strength of Test Specimens. The British Standards Institution: London, UK, 2009.
[18] ASTM International- ASTM C469/C469M-14; Standard Test Method for Static Modulus of Elasticity and Poisson's Ratio of Concrete in Compression. 04 (2014) 1–5.
[19] Van den Heever, M., "Experimental and Computational Mechanics for the Constitutive Modelling of Extrusion-based 3D Concrete Printing", PhD Dissertation in Engineering, Stellenbosch University, South Africa, (2021) 232 pp. https://scholar.sun.ac.za.
[20] Liang, J-Z., Predictions of Young's Modulus of Short Inorganic Fiber Reinforced Polymer Composites, Composites: Part B (2012), doi: 10.1016/j.compositesb.2012.01.010.